


Pretreatment with probiotic Bifico ameliorates colitis-associated cancer in mice: Transcriptome and gut flora profiling

Huan Song^{1,2}  | Weiyi Wang^{1,3} | Bo Shen¹ | Hao Jia² | Zhaoyuan Hou² | Ping Chen⁴ | Yunwei Sun¹

¹Department of Gastroenterology, Ruijin Hospital, Shanghai Jiaotong University School of Medicine, Shanghai, China

²Shanghai Key Laboratory for Tumor Microenvironment and Inflammation, Department of Biochemistry and Molecular Cellular Biology, Shanghai Jiaotong University School of Medicine, Shanghai, China

³Department of Endoscopy, Shanghai Eastern Hepatobiliary Surgery Hospital, Shanghai, China

⁴Department of Gastroenterology, Ruijin Hospital North, Shanghai Jiaotong University School of Medicine, Shanghai, China

Correspondence

Yunwei Sun, Department of Gastroenterology, Ruijin Hospital, Shanghai Jiaotong University School of Medicine, Shanghai, China.

Email: sunyunwei@aliyun.com

and

Ping Chen, Department of Gastroenterology, Ruijin Hospital North, Shanghai Jiaotong University School of Medicine, Shanghai, China.

Email: chenping714@aliyun.com

Funding information

Shanghai Municipal Population and Family Planning Commission, (XBR2013125) National Natural Science Foundation of China, (31601114, 31671415, 81072010, 81372309, 81402376).

Individuals with inflammatory bowel disease are at high risk of developing colitis-associated cancer (CAC). Strategies to block the process from inflammatory bowel disease to CAC should be considered. In the experiment, we aim to explore the chemopreventive efficacy of the probiotic cocktail Bifico and its potential mechanism in azoxymethane and dextran sodium sulphate-induced CAC in mice. Oral pretreatment of Bifico was adopted to evaluate its protective effect. The colorectums of 35 C57BL/6 mice were collected and examined for the degree of inflammation and tumorigenesis. Comparative 16S rRNA sequencing was carried out to observe Bifico-target alterations in gene expression and microbiota structure. We found that pretreatment of Bifico alleviated intestinal inflammation and reduced tumor formation. Furthermore, we identified a subset of genes as potential targets of Bifico treatment, including *CXCL1*, *CXCL2*, *CXCL3*, and *CXCL5*, which are all ligands of C-X-C motif receptor 2 (CXCR2). The 16S rRNA sequencing showed that Bifico decreased the abundance of genera *Desulfovibrio*, *Mucispirillum*, and *Odoribacter*, and a bloom of genus *Lactobacillus* was detected. Notably, we found that an abundance of these Bifico-target taxa was significantly associated with the expression of CXCR2 ligand genes. Our studies indicate that Bifico, given orally, can ameliorate CAC in mice through intervening with the possible link between *Desulfovibrio*, *Mucispirillum*, *Odoribacter*, *Lactobacillus*, and CXCR2 signaling.

KEYWORDS

carcinogenesis, chemokines, colorectal neoplasms, gastrointestinal microbiome

Abbreviations: AOM, azoxymethane; CAC, colitis-associated cancer; CCL, chemokine C-C motif ligand; CRC, colorectal cancer; Ctrl, Control; CXCL, chemokine C-X-C motif ligand; DSS, dextran sodium sulphate; IBD, inflammatory bowel disease; LDA, linear discriminant analysis; OTU, operational taxonomic unit; PGE₂, prostaglandin E₂; qPCR, quantitative PCR.

Huan Song and Weiyi Wang are contributed equally to this work.

This is an open access article under the terms of the Creative Commons Attribution-NonCommercial License, which permits use, distribution and reproduction in any medium, provided the original work is properly cited and is not used for commercial purposes.

© 2017 The Authors. *Cancer Science* published by John Wiley & Sons Australia, Ltd on behalf of Japanese Cancer Association.

1 | INTRODUCTION

It has been largely accepted that chronic inflammation is a pivotal causal component of somatic tumorigenesis and progression.^{1,2} A representative example of this strong association is colonic carcinogenesis arising in individuals with IBD.^{1,3-5} Colorectal cancer has been well studied and it can be divided into 2 types: colitis-associated CRC and sporadic CRC. Prolonged IBD is one of the major risks for CAC initiation, characterized by CAC incidence ranging from 2% after 10 years of IBD history up to 18% after 30 years.^{6,7} Considering the long course from IBD to CAC, there are opportunities for interventions to halt or even reverse the process of carcinogenesis in this high-risk population.⁸

Evidence is accumulating that dysbiosis of intestinal microbiota may greatly influence the pathogenesis of IBD and CRC in both animal models and humans.⁹⁻¹⁴ For example, bacterial phyla responsible for producing short-chain fatty acids are observed with decreased abundance in patients with IBD, which may serve as a cause or a consequence of permanent intestinal inflammation response in IBD.^{9,15,16} A recent study also reported that *Fusobacterium nucleatum* contributes to chemoresistance in CRC through modulating the network of Toll-like receptors, microRNAs, and autophagy.¹⁷ Thus, strategies of manipulating the gut flora to restore balance of the microbiota community may be therapeutically feasible in patients with IBD and CAC.

It has been reported by numerous studies that oral administration of probiotics VSL#3, a commercially available probiotic cocktail that contains 4 strains of genus *Lactobacillus*, 3 strains of genus *Bifidobacterium*, and 1 strain of genus *Streptococcus*, can reduce chronic inflammation and delay development of carcinoma in mouse models of CAC.^{13,18-20} However, conclusions on whether there is a therapeutic effect of probiotics on CAC are not exactly the same. The overwhelming majority of studies support the view that probiotics prevent inflammation and carcinogenesis.^{18,19,21} In contrast, a recent study reported that concurrent treatment with VSL#3 enhanced tumorigenesis in an AOM/Il10^{-/-} mouse model.²² Furthermore, the specific mechanisms underlying the beneficial effects of probiotics on CAC have not been fully investigated.

Bifico capsules were approved as an over-the-counter drug by the Chinese regulatory authority, the State Food and Drug Administration, in 2002.²³ Previous research has shown that Bifico could relieve gastritis induced by *Helicobacter pylori* and ameliorate experimental colitis caused by DSS in mice.^{24,25} However, the effect of Bifico on CAC has not been studied yet.

The goal of the present study is to evaluate the protective efficacy of Bifico capsules against AOM/DSS-induced CAC in mice. In addition, we identified several significantly altered gut bacterial groups and genes that were involved in the protective effect of Bifico treatment. Our results confirm that the probiotic cocktail Bifico has the capacity to restrain colonic carcinogenesis in mice, providing evidence for the clinical application of Bifico to lower the morbidity of CAC in patients with recurrent IBD.

2 | MATERIALS AND METHODS

2.1 | Experimental animals

Male C57BL/6 mice (age, 4 weeks) were purchased from the Laboratory of Animal Sciences, School of Medicine, Shanghai Jiao Tong University (Shanghai, China). The mice were specific pathogen-free and were bred and housed at the Animal Care Facility of the Ruijin Hospital, Shanghai Jiaotong University School of Medicine in laboratory conditions (23°C, 50% humidity, 12/12-h light/dark). The experiment protocol was approved by the Ethical Committee of Ruijin Hospital, Shanghai Jiaotong University School of Medicine.

2.2 | Reagents

Azoxymethane was purchased from Sigma-Aldrich (St. Louis, MO, USA) and DSS was purchased from MP Biomedicals (molecular weight, 36-50 kDa; Santa Ana, CA, USA). Bifico capsules, containing at least 1.0×10^7 c.f.u. viable lyophilized *Bifidobacterium longum*, 1.0×10^7 c.f.u. *Lactobacillus acidophilus*, and 1.0×10^7 c.f.u. *Enterococcus faecalis* for each capsule (210 mg), were gifts from Shanghai Sinepharm (Shanghai, China). Antibody against proliferating cell nuclear antigen was purchased from Cell Signaling Technology (Danvers, MA, USA).

2.3 | Experimental procedure

The experimental timeline of this experiment is shown in Figure 1. Thirty-five male C57BL/6 mice were randomly divided into 3 groups: the Ctrl group (n = 7), Model group (AOM/DSS only, n = 14), and Bifico group (n = 14). Modeling of CAC was carried out according to protocol.²⁶ The mice were injected i.p. with a single dose of AOM (10 mg/kg) on the first day and 3 cycles of DSS treatment was adopted thereafter. For each cycle of DSS, the mice in the Model and Bifico groups received water containing 2% DSS (w/v) for 7 days in a row, followed by 2 weeks of sterile water. The mice in the Bifico group were given Bifico capsules (4.2 g/kg, dissolved in 200 μ L physiological saline, at least 1.2×10^7 c.f.u./d per mouse) by lavage 2 weeks before the beginning of the experiment each day (10:00 AM) until the end of the experiment. The mice in the Ctrl and Model groups received the equivalent volume of physiological saline. Half of the mice in the Model and Bifico groups were randomly chosen to be killed by cervical dislocation (represented as Model 3 and Bifico 3 groups) at the end of week 3. Other mice were killed at the end of week 9 (represented as Model 9 group, Bifico 9 group, and Ctrl group).

2.4 | Histopathological evaluation and immunohistochemistry

Colon biopsies were macroscopically examined for tumorigenesis and were made as "Swiss-rolls".²⁶ The tissues were then fixed in

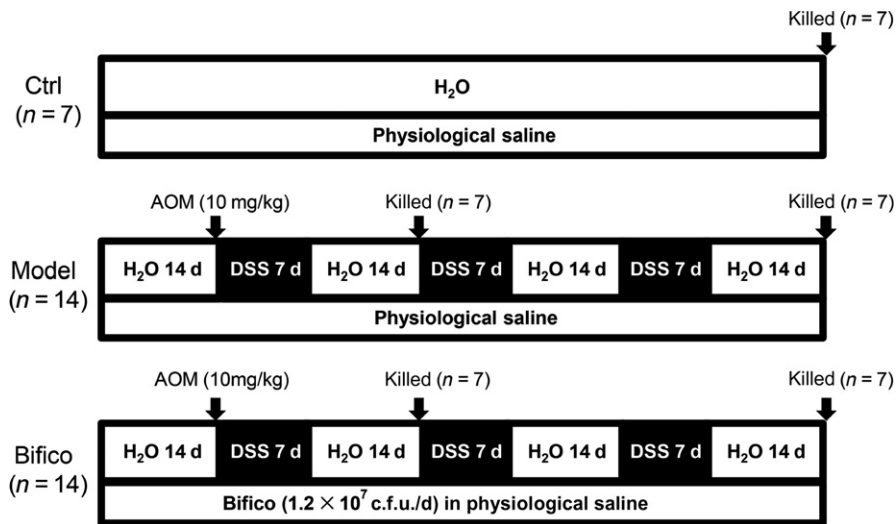


FIGURE 1 Experimental timeline for azoxymethane (AOM) and dextran sodium sulphate (DSS) mouse models of colitis-associated cancer with interventional administration of the probiotic cocktail Bifico. Ctrl, control; d, day

formalin overnight. The solution was subsequently changed to 70% ethanol before paraffin-embedding. The paraffin sections were stained with H&E in accordance with the standard procedures for histological evaluation.²⁶

2.5 | cDNA microarray

Total RNA was isolated from the colon tissues using TRIzol reagent (Invitrogen, Carlsbad, CA, USA) according to the manufacturer's protocols. Total RNA was extracted from colorectums of 12 mice in the Bifico 3, Model 3, Bifico 9, and Model 9 treatment groups ($n = 3/\text{group}$). The cDNA microarray analysis was carried out by Phalanx Biotech Group using OneArray (Mouse OneArray v2; Taiwan, China).

2.6 | DNA extraction and sequencing

Colons were removed and dissected longitudinally, then gently flushed with precooled PBS. Stools sticking on the mucosa were carefully removed using forceps. DNA was extracted using the QIAamp DNA MiniKit (Qiagen, Hilden, Germany). Polymerase chain reaction amplification of the 16S rRNA gene was carried out using PCR primers specific for the 338-806 (V3-V4) regions (338F, 5'-ACTCC-TACGGGAGGCAGC-3' and 806R, 5'-GGACTACHVGGGTWTCTAAT-3'). Purified amplicons were pooled in equimolar concentrations and paired-end sequenced on an Illumina MiSeq platform (Illumina, San Diego, CA, USA) at Majorbio Bio-Pharm Technology (Shanghai, China).

2.7 | Analysis of microbiota sequencing data

Operational taxonomic units were identified with a standard of at least 97% similarity in the 16S rRNA sequence using USEARCH and chimeric sequences were identified using UCHIME.^{27,28} Classification of representative reads for each OTU was carried out utilizing the RDP Classifier algorithm against the Silva 16S rRNA database with a confidence threshold of 0.7.^{29,30} The unweighted pair-group method with arithmetic mean was used for hierarchical clustering, and

principal co-ordinate analyses were performed with QIIME and R package software. A Venn diagram, bacterial taxonomic distributions, and Spearman's correlation coefficient were visualized using R software. Analysis of similarities was carried out using QIIME. Linear discriminant analysis effect size was undertaken to receive representative bacterial groups of the Bifico and Model groups.³¹

2.8 | Real-time qPCR

Total mRNA was extracted using TRIzol reagent (Invitrogen) and cDNA was synthesized using a PrimeScript RT reagent Kit (Takara Biotechnology, Dalian, China). Real-time qPCR was carried out using Hieff qPCR SYBR Green Master Mix (Yeasen, Shanghai, China) with the 7500 Real-Time PCR System (Applied Biosystems). The results were analyzed using the $2^{-\Delta\Delta CT}$ method. The primer sequences used in this experiment are shown in Table S1.

2.9 | Enzyme-linked immunosorbent assay

Levels of PGE₂ in the serum were assessed by double antibody sandwich ELISA Kits (Elabscience, Wuhan, China) according to the manufacturer's instructions.

2.10 | Statistics

Differences in expression of pro-inflammatory genes, tumor number, tumor average size, colon length, and richness of bacteria were analyzed by Student's *t* test using GraphPad Prism 7.0 software. Results were considered significant if two-tailed *P*-values were $< .05$.

3 | RESULTS

3.1 | Bifico treatment reduces colonic inflammation

The chemopreventive effect of Bifico against colonic inflammation was evaluated. The body weight of mice decreased substantially

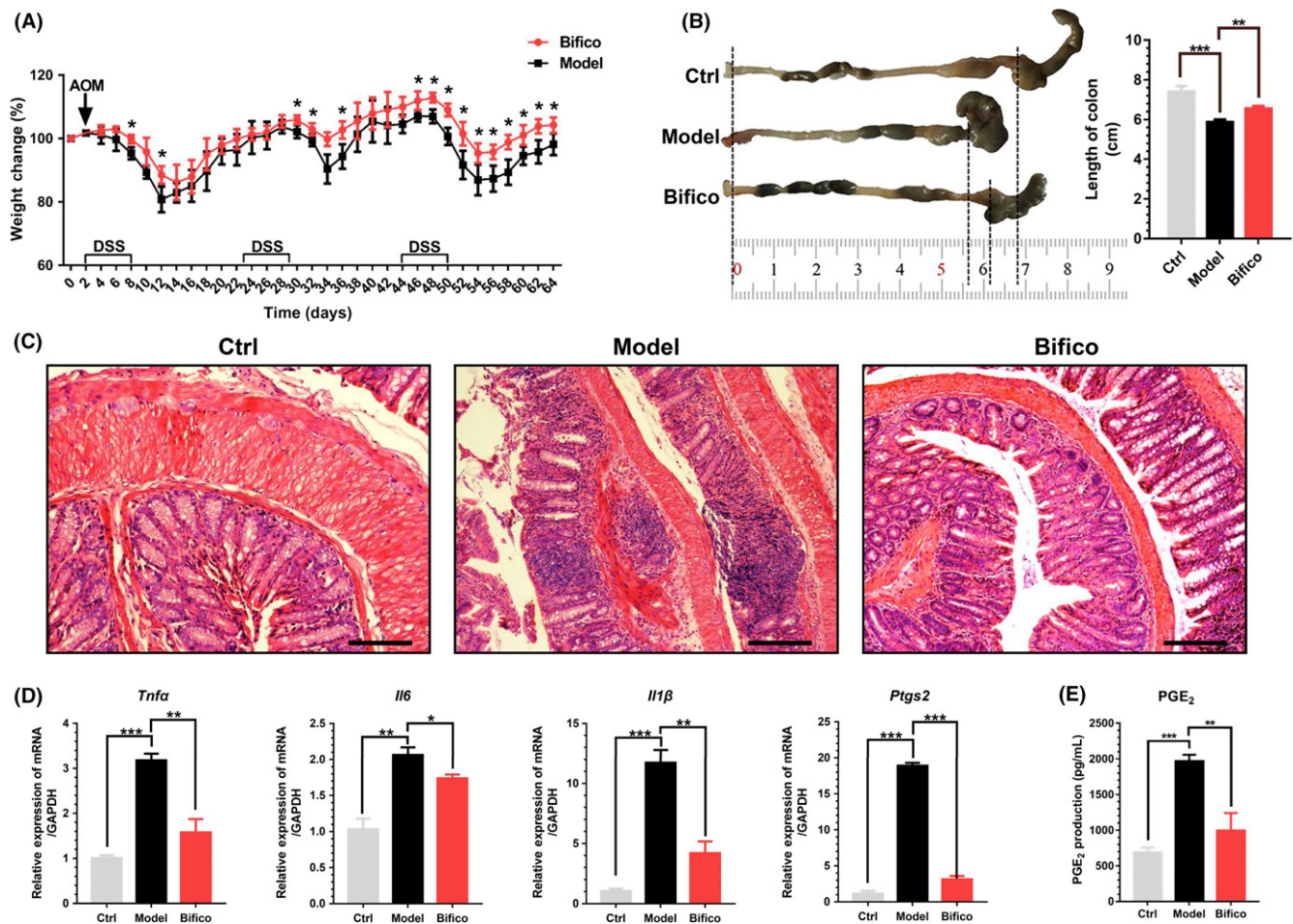


FIGURE 2 Treatment with probiotic Bifido alleviates colonic inflammation in azoxymethane (AOM) and dextran sodium sulphate (DSS)-induced mouse models of colitis-associated cancer. A, Weight changes over the whole period of the experiment. B, Representative images of colon morphology and statistics of colon length. C, Representative H&E histological sections of the colons. Original magnification, $\times 100$. D, Effect of Bifido on expression of pro-inflammatory genes in the colon tissues. E, Effect of Bifido on the level of prostaglandin E₂ (PGE₂) in the serum. Data are expressed as mean \pm SEM. * $P < .05$, ** $P < .01$, *** $P < .001$, compared to the Bifido group or the control (Ctrl) group ($n = 4$)

following each periodic exposure to DSS and the mice partially retrieved their body weight when DSS treatment was suspended. After the second exposure cycle to DSS, the body weight loss percentage of the mice in the Bifido group was significantly less extensive than the mice in the Model group (Figure 2A). Shortening of colon length was remarkably alleviated in response to Bifido treatment (Figure 2B). Colonic histological H&E stained sections showed the degree of colonic inflammation in each group (Figure 2C). Mucosal erosion, crypt distortion, inflammatory cell infiltration, and destruction of muscularis mucosae were observed (Figure 2C, Model and Bifido), and the impaired architecture of the colonic lamina propria was partly restored by Bifido treatment (Figure 2C, Bifido). There was no inflammatory damage present in mice of the Ctrl group (Figure 2C, Ctrl). Furthermore, the mRNA levels of pro-inflammatory genes were examined. The expression of *Tnfa*, *Il1β*, *Il6*, and *Ptgs1* dramatically increased due to treatment with AOM/DSS (Figure 2D). More noteworthy was that such an increment in expression levels of these genes was eliminated in mice of the Bifido group (Figure 2D). In addition, the level of PGE₂ in serum was measured. The

PGE₂ level was enhanced by AOM/DSS, and this enhancement was markedly inhibited by Bifido treatment (Figure 2E).

3.2 | Bifido treatment attenuates AOM/DSS-induced carcinogenesis

We observed occurrence of neoplastic lesions in response to AOM/DSS, and macroscopic images of the colorectums of mice among different groups are shown in Figure 3A. Most of the neoplasms were spread over the distal colon and rectum, ranging from 1 mm to 4 mm, with few tumors located in the proximal colon. Bifido treatment exerted a significant inhibitory effect on the multiplicity and size of colitis-induced tumors, with an average of 8.3 macroscopic tumors (mean diameter, 1.52 mm) per mouse in Bifido-treated animals vs 12.7 tumors (mean diameter, 1.23 mm) per mouse in the Model group (Figure 3B-E). In evaluation of colon histology, mice in the Model group showed evidence of multiple adenoma and invasive adenocarcinoma (Figure 3F, Model), whereas disease in mice in the Bifido group mainly manifested as crypt dysplasia and adenoma (Figure 3F, Bifido).

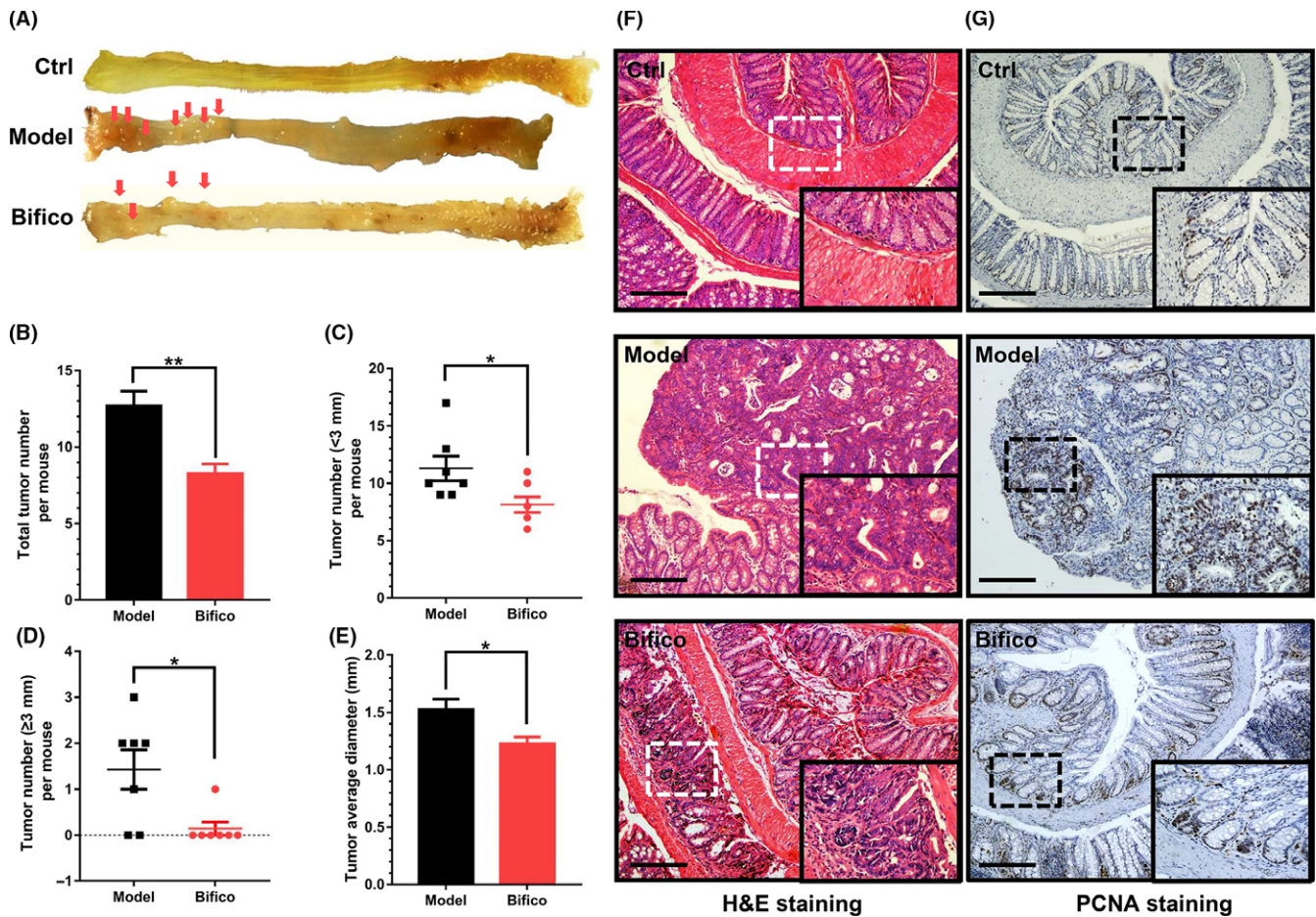


FIGURE 3 Chemopreventive effect of the probiotic cocktail Bifico on tumorigenesis in mouse models of colitis-associated cancer. A, Representative macroscopic imaging. Red arrows indicate tumors with diameter >1 mm. B–E, Statistics of tumor multiplicity, tumor diameter, and tumor distribution. F, G, Representative H&E sections of colons (F) and immunohistochemical staining with proliferating cell nuclear antigen (PCNA) (G). Data are expressed as mean \pm SEM ($n = 7$). $*P < .05$, $**P < .01$, compared to the Model group. Original magnification, $\times 100$; $\times 400$ for partial enlarged views in the bottom right corner of each image

Additionally, the expression of proliferating cell nuclear antigen was dramatically upregulated by AOM/DSS when compared with mice in the Ctrl group (Figure 3G, Model). Notably, this trend was significantly suppressed by Bifico treatment (Figure 3G, Bifico).

3.3 | Transcriptional changes induced by AOM/DSS and probiotic mixture treatment

To fully explore the underlying mechanism of the Bifico effect, global transcriptional changes of mice in the Model and Bifico groups were identified by cDNA microarray analysis of colon tissues. Two-dimensional hierarchical clustering showed distinct gene expression patterns at different time points among different groups (Figure S1). We compared gene expression levels of the mice in the Model group with those in the Bifico group. We identified 300 differentially expressed genes between mice in the Model and Bifico groups at week 9 (experiencing 3 DSS cycles), finding that 166 genes were upregulated and 134 genes were downregulated (\log_2 |fold change| ≥ 1.0 ; $P < .05$, marked as profile BIFICO). In addition, we were also interested in gene profile alterations during the process of

CAC progression. We compared the levels of gene expression at week 9 to those at week 3, and found that 1155 genes were upregulated, whereas 453 genes were downregulated (\log_2 |fold change| ≥ 1.0 ; $P < .05$, marked as profile CAC). We presented the above results with volcano plots (Figure S2A,B).

We then carried out biological pathway and gene ontology enrichment analyses using the Database for Annotation, Visualization and Integrated Discovery (<https://david.ncifcrf.gov/>) to identify possible biological pathways and biological processes associated with Bifico treatment.³² We undertook the enrichment analysis on the gene expression of profile BIFICO, and identified nine significantly canonical pathways. Figure 4A shows the significant pathways. We then continued to investigate significant canonical pathways associated with CAC progression by undertaking enrichment analysis on profile CAC. A total of 11 canonical pathways were identified (Figure 4B). The results of gene ontology enrichment analysis of profile BIFICO and profile CAC are displayed in Figure S2C,D.

Interestingly, we found some genes changed in the opposite direction according to the above results. To gain insight into the protective mechanism of Bifico, we compared significantly expressed

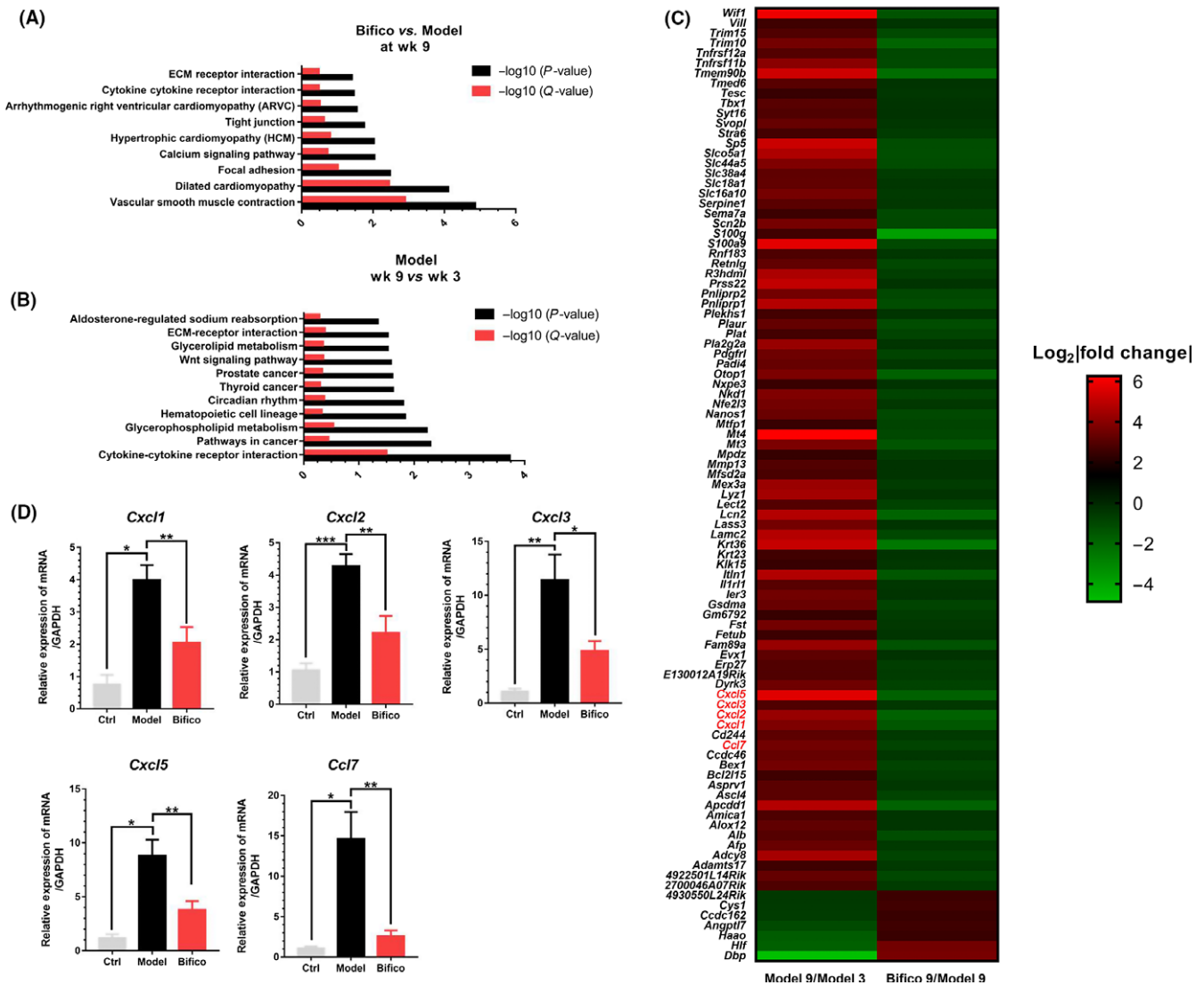


FIGURE 4 Results of cDNA microarray and validation of the expression of selected genes in azoxymethane (AOM) and dextran sodium sulphate (DSS)-induced mouse models of colitis-associated cancer. A, Significant canonical pathways of genes expressed differentially in response to treatment with the probiotic cocktail Bifico. B, Significant canonical pathways in progression of colitis-associated cancer. C, Bifico target genes ($n = 3$). D, Validation of the expression levels of selected genes; $n = 4$ mice/treatment group. Data are expressed as mean \pm SEM ($n = 4$). * $P < .05$, ** $P < .01$, *** $P < .001$, compared to the Bifico group or control (Ctrl) group. Bifico 9, mice treated with AOM/DSS and Bifico, killed at 9 wk; Model 3, mice treated with AOM/DSS without Bifico, killed at 3 wk; Model 9, mice treated with AOM/DSS without Bifico, killed at 9 wk

genes in the Model datasets at week 9 vs week 3 (profile CAC) and those in Bifico group vs Model group at week 9 (profile BIFICO). A total of 95 genes were found regulated in the opposite direction. We found that 88 genes upregulated by AOM/DSS were dramatically downregulated by Bifico, and another 7 genes changed in the opposite trend simultaneously ($\log_2[\text{fold change}] \geq 1.3$). Presumably, these genes could possibly serve as pivotal modulating factors in the preventive effect of Bifico against CAC progression (Figure 4C). Among the potential regulators, we selected 5 genes to validate their mRNA levels using RT-qPCR, including *CXCL1*, *CXCL2*, *CXCL3*, *CXCL5*, and *CCL7*. As presented in Figure 4D, fold changes of these genes in mice of the Bifico group were identified as significantly downregulated when compared with those in the Model group.

3.4 | Bifico alters composition of the mucosa-adherent microbiota community

To determine the changes in colonic microbiota community, we assessed the mucosa-adherent microbiota from colon tissues by using high-throughput sequencing. Microbial community diversity was estimated using the Chao1 and Shannon indices, and the richness was assessed based on the number of OTUs. Diversity of the gut flora was not significantly altered by Bifico treatment, although a lower trend in diversity in the intestinal microbiota of Bifico-fed mice was observed (Figure 5A). Similarity of the colonic flora among samples was revealed using a phylogenetic tree. Each branch of the tree represented the microbiota structure of 1 sample, and the

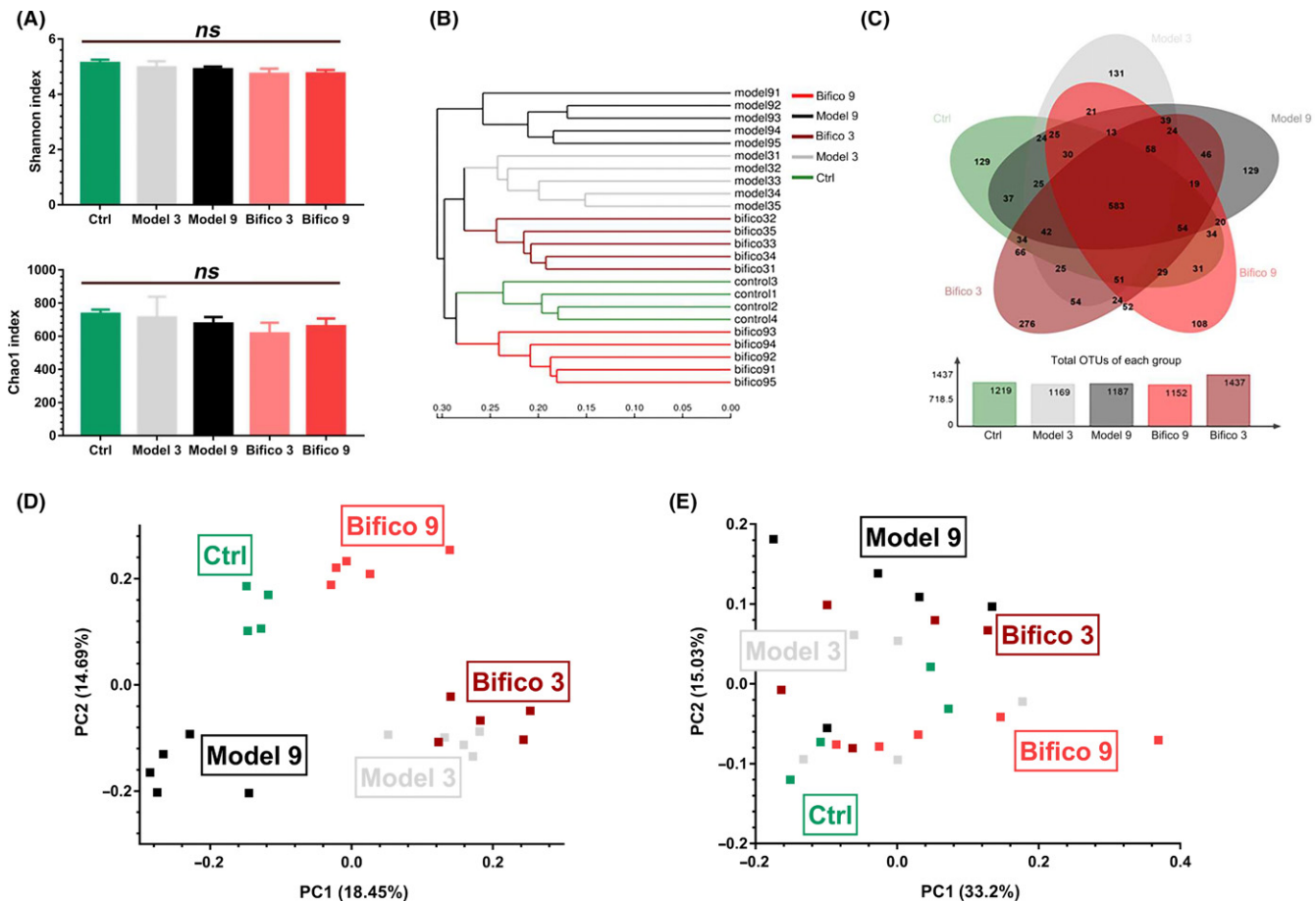


FIGURE 5 Bifido probiotic alters the community composition of mucosa-adherent microbiota in models of colitis-associated cancer. Mice were treated with azoxymethane and dextran sodium sulphate and killed at 3 wk or 9 wk (Model 3 and Model 9 groups, respectively), or also received Bifido (Bifico 3 and Bifico 9 groups, respectively); $n = 5$ mice/group. A, Bifido did not alter the Shannon index or Chao1 index. B, Hierarchical clustering tree for each sample at the operational taxonomic unit (OTU) level. C, Venn diagram of shared and unique OTUs among different groups. The histogram represents the number of OTUs of each group. D, E, Principal coordinates analysis based on Bray-Curtis dissimilarity (D) and weighted UniFrac dissimilarity (E). Control (Ctrl) group, $n = 4$. n.s., not significant

samples in the same group shared a high similarity (Figure 5B). Next, we examined the shared and unique bacterial OTUs among different groups. The shared OTUs from the 24 samples are shown with a Venn diagram (Figure 5C).

To obtain in-depth knowledge of changes of microbiota community structures caused by Bifido treatment, a principal co-ordinate analysis was carried out on Bray-Curtis dissimilarity and UniFrac weighted distance. Significant separation was revealed between Model and Bifido groups (analysis of similarity based on Bray-Curtis and weighted UniFrac distance; P -value, .006 and .014; Figure 5D,E, respectively).

3.5 | Bifido changes the abundance of specific taxa of the mucosal microbiota

Relative abundances of taxa (contributing $>1\%$) are depicted using pie charts in Figure 6A,B. Distribution of colonic microbiota in the Ctrl, Model 3, and Bifico 3 groups is shown with bar charts in

Figure S3. To explore the association between gut microbiota and the effect of Bifido, we further analyzed the changes on abundance of specific taxa. Bifido-treated mice showed a significant contraction of *Deferribacteres* in the mucosal microbiota (Figure 6A, Table S2). At the genus level, Bifido treatment resulted in a significant shrinkage of *Mucispirillum*, *Odoribacter*, and *Desulfovibrio* (Figure 6B, Table S3). Notably, Bifido treatment contributed to a significant increment of *Lactobacillus* (Figure 6B). We also attempted to identify the altered bacterial groups during the progression of CAC. *Mucispirillum*, *Odoribacter*, and *Desulfovibrio* were of increased abundance in Model 9 group, whereas *Ruminiclostridium* showed the opposite change (Figure S4).

To further determine the core bacterial group on the intestinal mucosa of mice, LDA coupled with effect size measurements was carried out ($P < .05$, LDA score >2.0). We found that 31 bacterial groups were enriched in the Model group, and 15 taxa in the Bifido treatment group (Figure 7A,B). Of all these bacterial groups, *Desulfovibrio*, *Mucispirillum*, and *Odoribacter* were the core genera

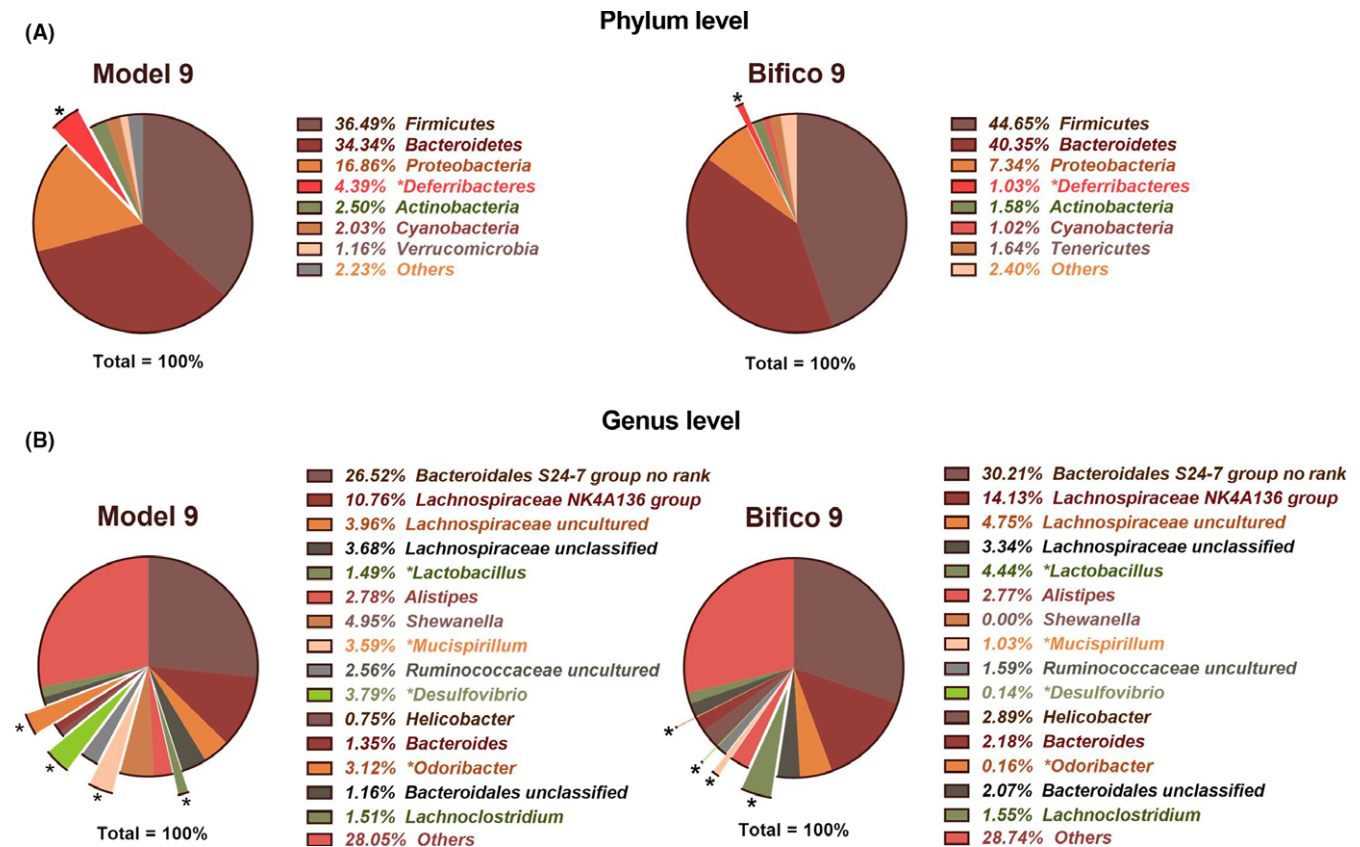


FIGURE 6 Bifico probiotic changes the structure of gut flora in models of colitis-associated cancer. Mice were treated with azoxymethane and dextran sodium sulphate and killed at 9 wk (Model 9 group), or also received Bifico (Bifico 9 group); $n = 5$ mice/group. Pie charts depict median standardized abundance (% of total) of the indicated taxa. A, B, Phylum level (A) and genus level (B) distribution of gut flora in Bifico 9 and Model 9 groups. Standardized abundance of taxa contributing $>1\%$ were included, and pair-wise comparisons were carried out using the Wilcoxon rank sum test. * $P < .05$

in the Model 9 group, whereas *Lactobacillus* was remarkably enriched in the Bifico 9 group (LDA score >4.0 ; Figure 7B).

3.6 | Changes in gene expression profiles are correlated with microbiota alterations

We selected 5 differentially expressed genes, concluded from results of the cDNA microarray, and quantified their expression changes (Figure 4D). More importantly, we found that some Bifico-influenced taxa were associated with these genes. Correlation between the relative abundance of the bacterial genus and the mRNA fold-change of selected genes of mice among the Bifico 9 and Model 9 groups are depicted utilizing a heat map of Spearman's correlation coefficients (Figure 7C). Taxa that were significantly associated with any of the 5 genes included *Desulfovibrio*, *Odoribacter*, *Mucispirillum*, and *Lactobacillus* (Figure 7C, Table S4). The bacterial groups that were of decreased abundance in the Bifico group, *Desulfovibrio* and *Odoribacter*, were positively correlated with expression of genes CXCL1, CXCL2, CXCL3, CXCL5, and CCL7, and *Mucispirillum* was positively associated with CXCL1, CXCL3, CXCL5, and CCL7 (Table S4). In contrast, *Lactobacillus* was negatively associated with the expression of CXCL2 and CCL7 (Table S4). Other correlated bacterial groups are

presented in Table S4. Similar correlations were observed at the OTU level (Table S5).

4 | DISCUSSION

It is universally accepted that alteration in the community structure of the microbiota acts as a driving force during the stepwise progression from inflammation to dysplasia to adenocarcinoma. Thus, the possibility of retraining tumor progression by manipulating the intestinal microbiota seems logical. In this experiment, we confirmed that prophylactic administration of Bifico could alleviate weight loss, reduce the multiplicity and average size of tumors, and lower the expression of pro-inflammatory genes in an AOM/DSS mouse model. These results are in agreement with numerous previous reports focusing on probiotics.^{18-20,33} Notably, compared with other studies focusing on VSL#3, we used a lower dose of probiotic (VSL#3 vs Bifico, 1×10^9 c.f.u. vs 1.2×10^7 c.f.u./mouse each day) to achieve a similar inhibitory effect on inflammation and tumorigenesis in an AOM/DSS mouse model, which reflects that *Lactobacillus*, *Bifidobacteria*, and *Enterococcus* could be an alternative combination, and a high dosage of probiotics may not be indispensable.

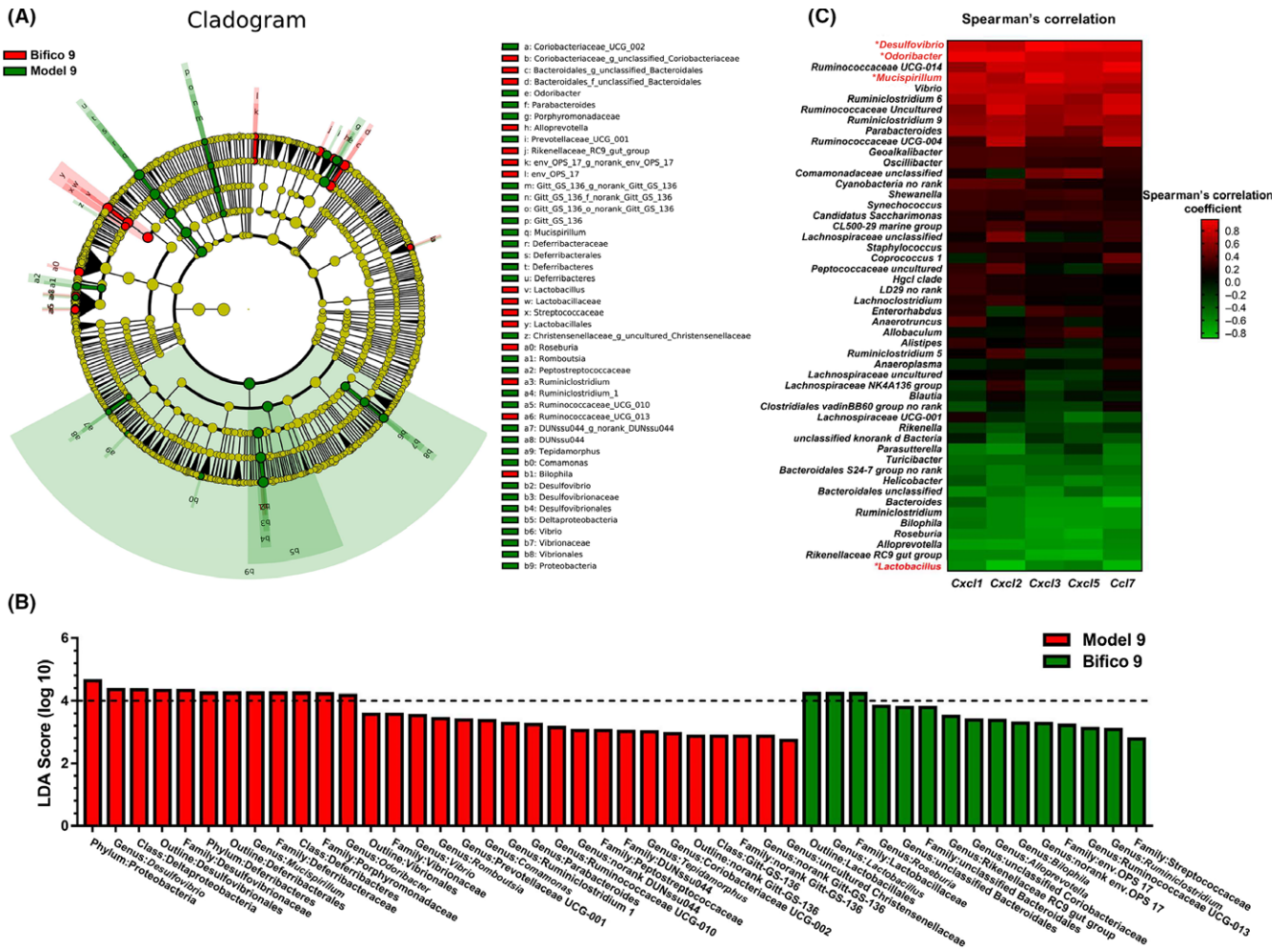


FIGURE 7 Cladogram, linear discriminant analysis (LDA) distribution, and heat map of Spearman's correlation coefficients of gut flora in models of colitis-associated cancer. Mice were treated with azoxymethane and dextran sodium sulphate and killed at 9 wk (Model 9 group), or also received the probiotic Bifico (Bifico 9 group). A, Taxonomic representation of taxa of the mice in Model and Bifico groups. B, Histogram of the LDA scores for differentially abundant microbiota. The threshold of LDA score was 2.0 ($n = 5$). C, Heat map of Spearman's correlation coefficients between expression of C-X-C motif receptor 2 signaling genes and relative abundance of Bifico target taxa. *Bacterial groups with LDA score >4.0 ($n = 4$)

To investigate the underlying mechanism of probiotics' preventive effect, we detected alterations in the gene expression profile and microbial community of the intestine. We compared gene expression profiles in the inflammatory phase (1 cycle of DSS) with that in the neoplastic phase (3 cycles of DSS), and canonical pathway analysis of these genes highlighted "cytokine-cytokine receptor interaction" as the most significantly influenced pathway induced by AOM/DSS, which is consistent with a previous study.³⁴ Most noteworthy was that this pathway also showed significance in a comparison of gene expression profiles between the Bifico group and the Model group, indicating that Bifico might exert preventive effects against tumorigenesis through reversing the expression of these genes.

CXCL1, CXCL2, CXCL3, and CXCL5 are all CXC chemokines with an Glu-Leu-Arg motif, and bind to CXCR2 to play their role.³⁵ CXCL1 and CXCL5 are reported to be significantly upregulated in human colorectal cancer specimens compared with their tumor adjacent

tissues.³⁶ CXCL1 contributes to tumor angiogenesis, cell invasion, and migration in several types of cancer, including colon cancer.^{5,37} In keeping with CXCL1 and CXCL5, CCL7 is also reported to enhance colon cancer progression and metastasis through epithelial-mesenchymal transition.³⁸ A previous study reported that deletion of CXCR2 can attenuate AOM/DSS-induced colitis-associated tumorigenesis through diminishing infiltration of granulocytic myeloid-derived suppressor cells.³⁵ Additionally, CXCR2 signaling can also enhance blood vessel formation in solid tumors through recruiting tumor-associated neutrophils.^{39,40} In our study, the gene expression of CXCR2 showed no difference between the Model and Bifico groups. However, CXCR2 ligands CXCL1, CXCL2, CXCL3, and CXCL5, which were significantly induced by AOM/DSS, were all markedly downregulated by Bifico treatment, indicating that Bifico might interfere with the migration of numerous types of tumor-infiltrating inflammatory cells and therefore reshape the tumor microenvironment to inhibit tumor progression.

Alternatively, Bifico could distinctly change the composition of the gut microbiota community attached to the colonic mucosa. As previous studies described, *Desulfovibrio* had the capacity to degrade sulfate and produce high levels of hydrogen sulfide, which is regarded as a genotoxic agent that might play a role in colitis and colonic tumorigenesis.⁴¹ *Desulfovibrio* also displays a flourish of relative abundance in IBD colon tissues and in patients with adenoma and rectal cancer.^{14,42-44} However, most studies have shown that the abundance of *Desulfovibrio* in the intestinal tract of colon cancer patients does not increase.^{45,46} Considering its role in triggering colonic inflammation, *Desulfovibrio* may be of larger significance in CAC initiation and progression than in sporadic colorectal cancer. Another putative mucin degrader, *Mucispirillum*, was detected at decreased levels in the Bifico-treated group when compared with the Model group.⁴⁷⁻⁴⁹ *Mucispirillum*, with increasing abundance in DSS-treated mice and natural killer T cell-deficient mice, is recognized as opportunistic pathogen that may fuel inflammation.^{14,47-49} *Odoribacter* is also reported to markedly bloom in AOM/DSS-induced CRC mice and patients with rectal cancer.^{42,50}

As shown in our results, the significant enrichment of *Desulfovibrio*, *Mucispirillum*, and *Odoribacter* in the Model group was partly removed by treatment with Bifico, suggesting that Bifico could relieve inflammation and decrease tumor formation by inhibiting these colitogenic bacteria. We also detected a tremendous expansion of the genus *Lactobacillus*, a member of the Bifico bacterial group. As reported by numerous studies, treatment with various strains of *Lactobacillus* reduces the severity of colitis and colitis-associated carcinogenesis in both mice and humans^{21,51-54} Therefore, we assume that *Lactobacillus* is the crucial component in Bifico's chemoprevention of colitis-associated tumorigenesis. Nevertheless, we did not detect any significant alteration in abundance of *Bifidobacteria* or *Enterococcus*, 2 other components in the Bifico cocktail, probably because we tested mucosa tissues rather than stool specimens, and the vast majority of the bacteria was excreted with feces.

Interestingly, we found that these CAC-associated bacterial taxa were correlated with the expression of CXCR2 signaling genes, which indicates a mechanistic link between CXCR2 signaling gene expression and alterations of certain bacterial groups. Such an association sustains the view that the microbiota could regulate the development of tumors through shaping the immune system.^{5,10} Presumably, *Desulfovibrio* and *Mucispirillum* may putatively degrade mucin, a component of the viscous-elastic mucus, and therefore impair its protection against external damage. Such a disruption of the intestinal barrier may directly lead to the consequence of increased exposure of the intestinal epithelial cells to the luminal microbiota. It is noteworthy that *Desulfovibrio* is reportedly capable of invading and surviving in KB cells, a kind of oral epidermoid carcinoma cell, thereby giving rise to increased production of interleukin-6 and interleukin-8.⁵⁵ We can speculate that *Desulfovibrio* might also trigger the inflammatory response through such a direct way in the process of CAC initiation and progression.

Notably, pathogenic bacteria groups are reported to induce expression of the inflammatory enzyme COX-2 in inflamed colonic mucosa.^{56,57} Both COX-2 and COX-2-derived PGE₂ have been

proven to upregulate CXCR2 ligands in intestinal mucosa and tumors.³⁵ Considering that the expression of COX-2 in the colon tissues and levels of PGE₂ in the serum were significantly downregulated by treatment with Bifico, we predict that COX-2 could be one of the mediators that links the altered colonic microbiota and the CXCR2 signaling axis in the Bifico intervention process.

Our results strongly suggest that the probiotic mixture Bifico exerted an efficacious chemopreventive impact on inflammation-associated CRC. Although we identified the noticeable changes in the global transcriptome and microbial community associated with probiotic treatment, the causal relationship between these changes and attenuated tumorigenesis cannot be determined. Further detailed studies are required to investigate this deeply. Most of all, our results imply a mechanistic link between the possible Bifico-responsive pathogenic taxa (*Desulfovibrio*, *Mucispirillum*, and *Odoribacter*) and the CXCR2 signaling axis during CAC progression, which could explain, in part, the pattern of the preventive effect of probiotic treatment.

ACKNOWLEDGMENTS

We thank all members of the Lab of Zhaoyuan Hou (Shanghai Key Laboratory for Tumor Microenvironment and Inflammation, Department of Biochemistry and Molecular Cellular Biology, Shanghai Jiaotong University School of Medicine, Shanghai) who helped with discussions and reviews of the manuscript. We thank Shanghai Sinepharm for its kind gift of Bifico capsules.

CONFLICT OF INTEREST

The authors have no conflict of interest.

ORCID

Huan Song  <http://orcid.org/0000-0001-5806-0928>

REFERENCES

1. Coussens LM, Werb Z. Inflammation and cancer. *Nature*. 2002;420:860-867.
2. Mantovani A. Cancer: inflammation by remote control. *Nature*. 2005;435:752-753.
3. Aggarwal BB, Shishodia S, Sandur SK, Pandey MK, Sethi G. Inflammation and cancer: how hot is the link? *Biochem Pharmacol*. 2006;72:1605-1621.
4. Grivennikov SI, Greten FR, Karin M. Immunity, inflammation, and cancer. *Cell*. 2010;140:883-899.
5. Wang D, Dubois RN, Richmond A. The role of chemokines in intestinal inflammation and cancer. *Curr Opin Pharmacol*. 2009;9:688-696.
6. Eisen GM, Chutkan R, Goldstein JL, et al. Guidelines for colorectal cancer screening and surveillance. *Gastrointest Endosc*. 2000;51:777-782.
7. Beaugerie L, Itzkowitz SH. Cancers complicating inflammatory bowel disease. *N Engl J Med*. 2015;372:1441-1452.
8. Maresso KC, Tsai KY, Brown PH, Szabo E, Lippman S, Hawk ET. Molecular cancer prevention: current status and future directions. *CA Cancer J Clin*. 2015;65:345-383.

9. Kostic AD, Xavier RJ, Gevers D. The microbiome in inflammatory bowel disease: current status and the future ahead. *Gastroenterology*. 2014;146:1489-1499.
10. Gagliani N, Hu B, Huber S, Elinav E, Flavell RA. The fire within: microbes inflame tumors. *Cell*. 2014;157:776-783.
11. Flemer B, Lynch DB, Brown JM, et al. Tumour-associated and non-tumour-associated microbiota in colorectal cancer. *Gut*. 2017;66:633-643.
12. Jostins L, Ripke S, Weersma RK, et al. Host-microbe interactions have shaped the genetic architecture of inflammatory bowel disease. *Nature*. 2012;491:119-124.
13. Bassaganya-Riera J, Viladomiu M, Pedragosa M, De Simone C, Hontecillas R. Immunoregulatory mechanisms underlying prevention of colitis-associated colorectal cancer by probiotic bacteria. *PLoS ONE*. 2012;7:e34676.
14. Rooks MG, Veiga P, Wardwell-Scott LH, et al. Gut microbiome composition and function in experimental colitis during active disease and treatment-induced remission. *ISME J*. 2014;8:1403-1417.
15. Machiels K, Joossens M, Sabino J, et al. A decrease of the butyrate-producing species *Roseburia hominis* and *Faecalibacterium prausnitzii* defines dysbiosis in patients with ulcerative colitis. *Gut*. 2014;63:1275.
16. Morgan XC, Tickle TL, Sokol H, et al. Dysfunction of the intestinal microbiome in inflammatory bowel disease and treatment. *Genome Biol*. 2012;13:R79.
17. Yu T, Guo F, Yu Y, et al. *Fusobacterium nucleatum* promotes chemoresistance to colorectal cancer by modulating autophagy. *Cell*. 2017;170:548-563 e16.
18. Appleyard CB, Cruz ML, Isidro AA, Arthur JC, Jobin C, De Simone C. Pretreatment with the probiotic VSL#3 delays transition from inflammation to dysplasia in a rat model of colitis-associated cancer. *Am J Physiol Gastrointest Liver Physiol*. 2011;301:G1004-G1013.
19. Talero E, Bolivar S, Avila-Roman J, Alcaide A, Fiorucci S, Motilva V. Inhibition of chronic ulcerative colitis-associated adenocarcinoma development in mice by VSL#3. *Inflamm Bowel Dis*. 2015;21:1027-1037.
20. Do EJ, Hwang SW, Kim SY, et al. Suppression of colitis-associated carcinogenesis through modulation of IL-6/STAT3 pathway by balsalazide and VSL#3. *J Gastroenterol Hepatol*. 2016;31:1453-1461.
21. Zhang Y, Ma C, Zhao J, Xu H, Hou Q, Zhang H. *Lactobacillus casei* Zhang and vitamin K2 prevent intestinal tumorigenesis in mice via adiponectin-elevated different signaling pathways. *Oncotarget*. 2017;8:24719-24727.
22. Arthur JC, Gharaibeh RZ, Uronis JM, et al. VSL#3 probiotic modifies mucosal microbial composition but does not reduce colitis-associated colorectal cancer. *Sci Rep*. 2013;3:2868.
23. Yu H, Liu L, Chang Z, et al. Genome sequence of the bacterium *Bifidobacterium longum* strain CMCC P0001, a probiotic strain used for treating gastrointestinal disease. *Genome Announc*. 2013;1:e00716-13.
24. Yu HJ, Liu W, Chang Z, et al. Probiotic BIFICO cocktail ameliorates *Helicobacter pylori* induced gastritis. *World J Gastroenterol*. 2015;21:6561-6571.
25. Zhao HM, Huang XY, Zuo ZQ, et al. Probiotics increase T regulatory cells and reduce severity of experimental colitis in mice. *World J Gastroenterol*. 2013;19:742-749.
26. Thaker AI, Shaker A, Rao MS, Ciorba MA. Modeling colitis-associated cancer with azoxymethane (AOM) and dextran sulfate sodium (DSS). *J Vis Exp*. 2012;11:e4100.
27. Edgar RC. Search and clustering orders of magnitude faster than BLAST. *Bioinformatics*. 2010;26:2460.
28. Edgar RC, Haas BJ, Clemente JC, Quince C, Knight R. UCHIME improves sensitivity and speed of chimera detection. *Bioinformatics*. 2011;27:2194-2200.
29. Quast C, Pruesse E, Yilmaz P, et al. The SILVA ribosomal RNA gene database project: improved data processing and web-based tools. *Nucleic Acids Res*. 2013;41:D590.
30. Wang Q, Garrity GM, Tiedje JM, Cole JR. Naïve bayesian classifier for rapid assignment of rRNA sequences into the new bacterial taxonomy. *Appl Environ Microbiol*. 2007;73:5261.
31. Segata N, Izard J, Waldron L, et al. Metagenomic biomarker discovery and explanation. *Genome Biol*. 2011;12:R60.
32. Huang DW, Sherman BT, Lempicki RA. Systematic and integrative analysis of large gene lists using DAVID bioinformatics resources. *Nat Protoc*. 2009;4:44.
33. Kim SW, Kim HM, Yang KM, et al. *Bifidobacterium lactis* inhibits NF-kappaB in intestinal epithelial cells and prevents acute colitis and colitis-associated colon cancer in mice. *Inflamm Bowel Dis*. 2010;16:1514-1525.
34. Guo Y, Su ZY, Zhang C, et al. Mechanisms of colitis-accelerated colon carcinogenesis and its prevention with the combination of aspirin and curcumin: transcriptomic analysis using RNA-seq. *Biochem Pharmacol*. 2017;135:22-34.
35. Katoh H, Wang D, Daikoku T, Sun H, Dey SK, Dubois RN. CXCR2-expressing myeloid-derived suppressor cells are essential to promote colitis-associated tumorigenesis. *Cancer Cell*. 2013;24:631-644.
36. Rubie C, Frick VO, Wagner M, et al. ELR+ CXC chemokine expression in benign and malignant colorectal conditions. *BMC Cancer*. 2008;8:178.
37. Acharyya S, Oskarsson T, Vanharanta S, et al. A CXCL1 paracrine network links cancer chemoresistance and metastasis. *Cell*. 2012;150:165-178.
38. Lee YS, Kim SY, Song SJ, et al. Crosstalk between CCL7 and CCR3 promotes metastasis of colon cancer cells via ERK-JNK signaling pathways. *Oncotarget*. 2016;7:36842-36853.
39. Tazzyman S, Lewis CE, Murdoch C. Neutrophils: key mediators of tumour angiogenesis. *Int J Exp Pathol*. 2009;90:222-231.
40. Jablonska J, Wu CF, Andzinski L, Leschner S, Weiss S. CXCR2-mediated tumor-associated neutrophil recruitment is regulated by IFN-beta. *Int J Cancer*. 2014;134:1346-1358.
41. Singh SB, Lin HC. Hydrogen sulfide in physiology and diseases of the digestive tract. *Microorganisms*. 2015;3:866-889.
42. Thomas AM, Jesus EC, Lopes A, et al. Tissue-associated bacterial alterations in rectal carcinoma patients revealed by 16S rRNA community profiling. *Front Cell Infect Microbiol*. 2016;6:179.
43. Hale VL, Chen J, Johnson S, et al. Shifts in the fecal microbiota associated with adenomatous polyps. *Cancer Epidemiol Biomarkers Prev*. 2017;26:85-94.
44. Rowan F, Docherty NG, Murphy M, Murphy B, Calvin Coffey J, O'Connell PR. *Desulfovibrio* bacterial species are increased in ulcerative colitis. *Dis Colon Rectum*. 2010;53:1530-1536.
45. Balamurugan R, Rajendiran E, George S, Samuel GV, Ramakrishna BS. Real-time polymerase chain reaction quantification of specific butyrate-producing bacteria, *Desulfovibrio* and *Enterococcus faecalis* in the feces of patients with colorectal cancer. *J Gastroenterol Hepatol*. 2008;23(8 Pt 1):1298-1303.
46. Scanlan PD, Shanahan F, Marchesi JR. Culture-independent analysis of *desulfovibrios* in the human distal colon of healthy, colorectal cancer and polypectomized individuals. *FEMS Microbiol Ecol*. 2009;69:213-221.
47. Selvanantham T, Lin Q, Guo CX, et al. NKT cell-deficient mice harbor an altered microbiota that fuels intestinal inflammation during chemically induced colitis. *J Immunol*. 2016;197:4464-4472.
48. Berry D, Schwab C, Milinovich G, et al. Phylotype-level 16S rRNA analysis reveals new bacterial indicators of health state in acute murine colitis. *ISME J*. 2012;6:2091-2106.
49. Berry D, Kuzyk O, Rauch I, et al. Intestinal microbiota signatures associated with inflammation history in mice experiencing recurring colitis. *Front Microbiol*. 2015;6:1408.

50. Zackular JP, Baxter NT, Iverson KD, et al. The gut microbiome modulates colon tumorigenesis. *MBio*. 2013;4:e00692-13.
51. Irecta-Najera CA, Del Rosario Huizar-Lopez M, Casas-Solis J, Castro-Felix P, Santerre A. Protective effect of *Lactobacillus casei* on DMH-induced colon carcinogenesis in mice. *Probiotics Antimicrob Proteins*. 2017;9:163-171.
52. Verma A, Shukla G. Probiotics *Lactobacillus rhamnosus* GG, *Lactobacillus acidophilus* suppresses DMH-induced procarcinogenic fecal enzymes and preneoplastic aberrant crypt foci in early colon carcinogenesis in Sprague Dawley rats. *Nutr Cancer*. 2013;65:84.
53. von Schillde MA, Hörmannspurger G, Weiher M, et al. Lactocepine secreted by *Lactobacillus* exerts anti-inflammatory effects by selectively degrading proinflammatory chemokines. *Cell Host Microbe*. 2013;11:387-396.
54. Tang C, Kamiya T, Liu Y, et al. Inhibition of dectin-1 signaling ameliorates colitis by inducing *Lactobacillus*-mediated regulatory T cell expansion in the intestine. *Cell Host Microbe*. 2015;18:183.
55. Bissonboutelliez C, Massin F, Dumas D, Miller N, Lozniewski A. *Desulfovibrio* spp. survive within KB cells and modulate inflammatory responses. *Oral Microbiol Immunol*. 2010;25:226-235.
56. Abdallah Hajj Hussein I, Freund JN, Reimund JM, et al. Enteropathogenic *E. coli* sustains iodoacetamide-induced ulcerative colitis-like colitis in rats: modulation of IL-1 β , IL-6, TNF- α , COX-2, and apoptosis. *J Biol Regul Homeost Agents*. 2012;26:515.
57. Lee IA, Kim DH. *Klebsiella pneumoniae* increases the risk of inflammation and colitis in a murine model of intestinal bowel disease. *Scand J Gastroenterol*. 2011;46:684-693.

SUPPORTING INFORMATION

Additional Supporting Information may be found online in the supporting information tab for this article.

How to cite this article: Song H, Wang W, Shen B, et al. Pretreatment with probiotic Bifico ameliorates colitis-associated cancer in mice: Transcriptome and gut flora profiling. *Cancer Sci*. 2018;109:666–677. <https://doi.org/10.1111/cas.13497>